Journal of Colloid and Interface Science 461 (2016) 352–358

Contents lists available at ScienceDirect

Journal of Colloid and Interface Science

journal homepage: www.elsevier.com/locate/jcis

Enhanced perfume surface delivery to interfaces using surfactant surface multilayer structures

Robert Brabury [a,1], Jeffrey Penfold [a,b,*], Robert K. Thomas [a], Ian M. Tucker [c], Jordan T. Petkov [c,2], Craig Jones [c]

[a] Physical and Theoretical Chemistry Laboratory, South Parks Road, Oxford, UK
[b] STFC, Rutherford Appleton Laboratory, Chilton, Didcot, Oxon, UK
[c] Unilever Research and Development Laboratory, Port Sunlight, Quarry Road East, Bebington, Wirral, UK

HIGHLIGHTS

- Surface multilayer formation enhances perfume adsorption.
- Linalool and phenylethanol located in different regions.
- Linalool solubilized into alkyl chain region.
- Phenylethanol solubilized into headgroup region.
- Systems have potential for enhanced surface delivery and retention.

GRAPHICAL ABSTRACT

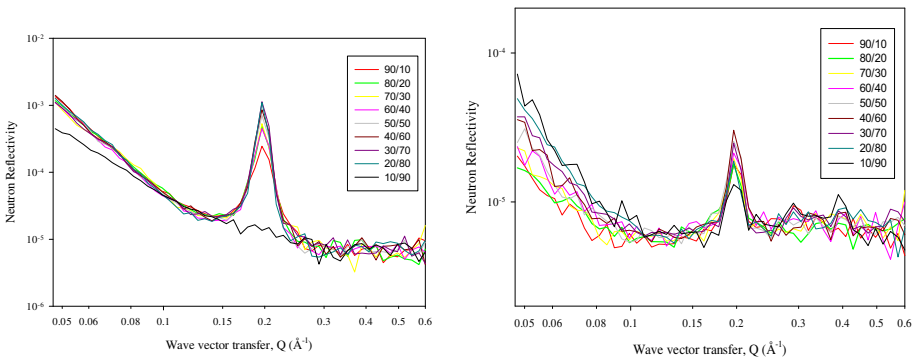

ARTICLE INFO

Article history:
Received 2 September 2015
Revised 17 September 2015
Accepted 18 September 2015
Available online 21 September 2015

Keywords:
Surfactant multilayers
Model perfumes
Adsorption

ABSTRACT

Enhanced surface delivery and retention of perfumes at interfaces are the keys to their more effective and efficient deployment in a wide range of home and personal care related formulations. It has been previously demonstrated that the addition of multivalent counterions, notably Ca^{2+}, induces multilayer adsorption at the air–water interface for the anionic surfactant, sodium dodecyl-6-benzenesulfonate, LAS-6. Neutron reflectivity, NR, measurements are reported here which demonstrate that such surfactant surface multilayer structures are a potentially promising vehicle for enhanced delivery of perfumes to interfaces. The data show that the incorporation of the model perfumes, phenylethanol, PE, and linalool, LL, into the surface multilayer structure formed by LAS-6/Ca^{2+} results in the surface structures being retained up to relatively high perfume mole fractions. Furthermore the amount of perfume at the surface is enhanced by at least an order of magnitude, compared to that co-adsorbed with a surfactant monolayer.

1. Introduction

Perfumes are important ingredients in a wide range of surfactant based home and personal care products [1–3]. Surface delivery and retention, evaporation into the vapor phase, and the impact upon surfactant self-assembly are the main elements of perfume performance. In particular enhancing surface delivery and retention of

* Corresponding author at: STFC, Rutherford Appleton Laboratory, Chilton, Didcot, Oxon, UK.
E-mail address: jeff.penfold@stfc.ac.uk (J. Penfold).
[1] Current address: Centre for Exploitation of Energy and Matter, Dept of Physics, Indiana University, Bloomington, IN, USA.
[2] Current address: KLK Oleo, SDN BHD, Menara KLK, Mutiara Damansara, 47810 Petaling, Jaya Selanger, Malaysia.

http://dx.doi.org/10.1016/j.jcis.2015.09.045
0021-9797/

perfumes at interfaces are the keys to their more effective and efficient deployment in home and personal care formulations. A wide range of model perfume molecules with differing degrees of solubility and hydrophobicity have been studied, and include fragrance components such as phenyl ethanol, limonene, linalool, geraniol and eugenol. These studies have largely focused on aspects such as the solubilization in different surfactant systems [4–8], the location of the perfume molecule within the self-assembled structure [9], and their impact upon surfactant phase behavior [10–12]. In contrast there have been relatively few studies which have directly probed the co-adsorption of perfumes with surfactants at interfaces, or investigations in which the adsorption can be enhanced.

However a number of different approaches for enhanced perfume solubilization, delivery and retention have been proposed and exploited; and include the use of micro-encapsulates, microemulsions, and other nano-particles, and polymer–surfactant mixtures [13,14]. Goddard and Gruber [15] discussed the application of polymer–surfactant mixtures to deliver flavors, colorants, perfumes and biologically active ingredients to interfaces, where the enhanced surface activities of polymer–surfactant mixtures and synergies in solubilization of perfumes may lead to enhanced surface delivery [16–18]. The synergies in surface activities in mixed surfactants have also been the focus of increased perfume solubilization [5,7]. Somasundaran et al. [19] have discussed the role of surfactant and polymer based nanoparticles and nanogels in personal care applications and solubilization slow release of fragrances. Indeed different forms of micro-encapsulates have demonstrated potential in perfume solubilization and delivery [20,21], and in applications requiring sustained release [22]. Binks et al. [23] have investigated the relative retardation of perfume evaporation from oil-in-water emulsions stabilized by either surfactant or nanoparticles. Bradbury et al. [24] have demonstrated how the strong surface interaction between polyelectrolytes and ionic surfactants can be used to manipulate surfactant adsorption and how the specific interaction between ionic surfactants and perfumes can enhance adsorption [25].

Surfactant surface multilayer formation has been demonstrated in relative dilute surfactant systems with the addition of multivalent counterions or polyelectrolytes [26]. Of particular relevance to this work is the surface multilayer formation for sodium dodecyl-6-benzenesulfonate, LAS-6, with $CaCl_2$ [27] and for sodium dodecyldioxyethylenesulfate, SLES, with $AlCl_3$ [28]. Depending on the surfactant and counterion concentrations surface multilayer structures with numbers of bilayers ranging from 1 to >30 can be formed at the surface. The focus of this paper is to explore the extent to which model perfumes can be incorporated into those surface multilayer structures without causing the surface structure to disassemble. This would provide a potentially novel route to obtaining enhanced surface adsorption and retention of perfumes at interfaces.

The paper describes the formation of surface multilayer structures for LAS-6 in the presence of Ca^{2+} counterions at relatively low surfactant concentrations, 2 mM, and their characterization using neutron reflectivity, NR. The impact of the addition of increasing amounts of two model perfumes, phenylethanol, PE, and linalool, LL, where PE is more soluble and hydrophilic than LL, on the surface structure is followed by NR. Using deuterium labeled surfactant and perfumes the distribution of both components at the interface is determined.

2. Experimental details

2.1. Neutron reflectivity

The neutron reflectivity measurements were made at the air–water interface on the SURF reflectometer at the ISIS pulsed neutron source in the UK [29]. The reflectivity, $R(Q)$ was measured as a function of the wave vector transfer, Q, in the direction normal to the surface (where Q is defined as $Q = 4\pi\sin\theta/\lambda$, θ is the grazing angle of incidence and λ is the neutron wavelength). The neutron beam was incident at a θ of 1.5°, and neutron wavelengths from 1 to 7 Å were used to cover a Q range of 0.048–0.5 $Å^{-1}$. The samples were aligned and the data corrected and normalized using established procedures. The measurements were made at a constant temperature of 25 °C and the samples (with a total volume ~25 ml) were contained in stainless steel troughs. Previous measurements in Teflon troughs [30] have established that preferential adsorption of the perfume components to the Teflon surface can substantially affect the adsorption to the air–water interface. The measurements were made initially for the LAS-6/$CaCl_2$ mixture, and when the surface multilayer structure reached equilibrium (after ~60 to 90 min) the perfume was added progressively using a micro-pipette. Each individual NR measurement took ~30 to 60 min. Some repeated measurements were made to ensure that equilibrium was reached. This occurred within the timescale of the measurements, and no differences in equilibration time were observed between linalool and phenylethanol. The NR measurements were made for isotopic combinations of deuterated surfactant/protonated perfume, and hydrogeneous surfactant/deuterated perfume in null reflecting water, nrw (92 mol% H_2O – 8 mol% D_2O has a scattering length of zero, the same as air). In such cases the reflectivity arises predominantly from the adsorbed layer of deuterated material at the interface. This approach is the basis of extensive measurements of surfactant and mixed surfactant adsorption reported in the recent literature [31]. The neutron scattering lengths, associated with each component used, are listed in Table 1.

2.2. Materials

The anionic surfactant LAS, sodium dodecyl-6-benzenesulphonate, was custom synthesized at Oxford and Unilever Research and Development [27] as the near symmetrical isomer with the phenyl ring joined at the middle of the C_{12} alkyl chain (C_6 position) and is referred to here as LAS-6. This applies to both the hydrogeneous and deuterated surfactant, and for the deuterated surfactant the alkyl chain and phenyl ring were both deuterium labeled. Two different isotopic forms of PE and LL were used, h-PE, d_5-PE, and h-LL, d_{11}-LL. The h-PE was obtained from Sigma Aldrich and the d_5-PE from CDN Isotopes, both with a purity of 98%, and were used as supplied. The h-LL was obtained from Sigma–Aldrich with a purity of 97% and used as supplied. The deuterated LL was synthesized at Unilever R&D [32]. The structure of the surfactant and perfumes are shown in Fig. 1.

Calcium chloride was obtained in dehydrate form from Sigma–Aldrich at 99% purity and was used as purchased. UHQ (Elga Ultrapure) water and D_2O, obtained from Sigma–Aldrich, were used throughout. The stainless steel troughs and all associated glassware were cleaned in Decon 90 and rinsed in UHQ thoroughly.

3. Results and discussion

3.1. LAS-6/$CaCl_2$

Prior to the addition of the perfumes (PE or LL) NR measurements were made for 2 mM LAS-6 in 1 mM $CaCl_2$, to characterize the surface structure in the absence of perfume. The NR data are shown in Fig. 2 for d-LAS-6 in nrw, and are characterized by a single Bragg peak at a Q of ~0.2 $Å^{-1}$.

The data are consistent with that previously reported for LAS-6/$CaCl_2$ [25], and are modeled using a previously described approach

Table 1
Neutron scattering lengths, molecular weight, and molecular volumes for the different components used in this study.

Component	Molecular formula	Molecular mass (g mol^{-1})	Molecular volume (Å^3)	Sum of scattering lengths, Σb (Å)
h-LAS-6	$C_{18}H_{29}SO_3Na$	348	567	3.51×10^{-4}
d-LAS-6	$C_{18}D_{29}SO_3Na$	377		3.37×10^{-3}
h-Phenylethanol	C_8H_9OH	122	198	2.16×10^{-4}
d_5-Phenylethanol	$C_8D_5H_4OH$	127		7.37×10^{-4}
h-Linalool	$C_{10}H_{17}OH$	154	340	4.95×10^{-5}
d_{11}-Linalool	$C_{10}D_{11}H_6OH$	165		1.2×10^{-3}

[27,28]. Within the kinematic approximation, and using an approach based on the work of Tidswell et al. [33] and Sinha et al. [34] the specular reflectivity for multilayers at the interface can be written as,

$$R(Q) = \frac{16\pi^2}{Q^4}\left|\sum_{i-0}^{2N}(\rho_i - \rho_{i+1})\exp(-iQd_i)\exp\left(\frac{-Q^2\sigma^2}{2}\right)\right|^2 \quad (1)$$

where ρ_i is the scattering length density of the ith layer, $i = 0$ represent the subphase, d_i is the distance between the interfaces between the ith and $(i+1)$th layers from the subphase, $d_i = \Sigma_i l_i$, l_i is the thickness of the ith layer, σ_i is the roughness of the ith to $(i+1)$th interface, $\rho(N+1)$ is the scattering length density of the upper bulk phase, and $2N$ is the number of layers (N is the number of bilayers). In the context of the application of Eq. (1) to the NR data the key model parameters are N the number of bilayers, d_t the bilayer thickness (where $d_t = d_1 + d_2$, and d_1 and d_2 are the thicknesses of the alkyl chain and headgroup regions of the bilayer), ρ_1 and ρ_2 (the scattering length densities associated with d_1 and d_2). There is an additional resolution term, ΔQ, which accounts for the instrumental resolution in Q but also has an additional contribution which represents, by analogy with crystalline materials, the mosaic spread in the bilayer stacks at the interface.

The position of the Bragg peak in Q is determined by d_t and its width by a combination of N (in the absence of a contribution from resolution the width is inversely proportional to N) and ΔQ. The intensity of the Bragg peak is related primarily to N and $\Delta\rho$ $(\rho_1 - \rho_2)$, and the form of the reflectivity at lower Q values (below the Bragg peak) is related to N and $(\rho_1 + \rho_2)$. Taking these factors into account yields the following key model parameters for the model fit in Fig. 1, with $d_t = 31.5 \pm 0.5$ Å, ($d_1 = 17.5 \pm 0.5$, $d_2 = 14 \pm 0.5$ Å), ρ_1 and $\rho_2 = 5 \pm 0.05 \times 10^{-6}$ and $3.6 \pm 0.05 \times 10^{-6}$ Å^{-2} respectively, $N = 30 \pm 5$, and $\Delta Q = 0.1 \pm 0.02$; and this provides a good description of the data. However N, $\Delta\rho$ and ΔQ are not entirely independent and so should be considered as approximate values consistent with the data.

Although d_t is well determined from the Q value of the 1st order Bragg peak the values of d_1 and d_2 are less well defined when only a single Bragg peak is visible. In this case d_1 and d_2 are largely chosen to be consistent with the molecular dimensions. That is, d_1 is assumed to contain the alkyl chains, and $2 \times l_c$ (where l_c is the fully extended length for a di-C_6 chain) is ~18 Å. Assuming then that d_2 contains the phenyl ring, the sulfonate headgroup and some hydration, d_2 would

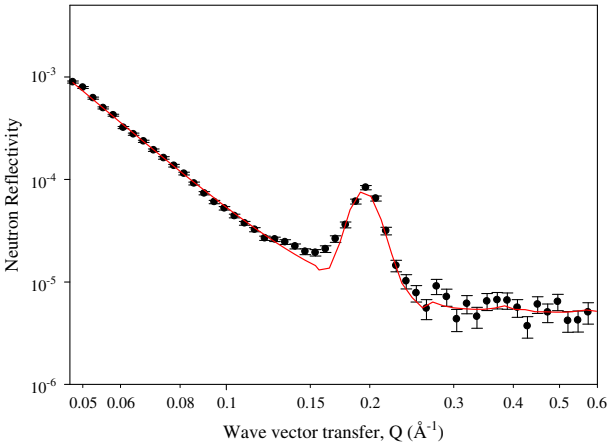

Fig. 2. NR data for 2 mM d-lAS-6/nrw and 1 mM $CaCl_2$. The solid line is a model fit for a multilayer structure at the interface, using the model and model parameters described in the main text.

be ~12 Å (with 4 Å for the phenyl ring and 2 Å for the sulfonate group). On this basis, the values of ρ_1 and ρ_2 then give an area/molecule within the bilayer stack ~50 ± 5 Å^2 (these values are calculated on the established basis that in nrw the area/molecule within an surfactant layer is given by $A = \sum b/d\rho$ [31]). Hence the model parameters are consistent with the associated molecular dimensions and deuterium labeling. This has important implications for the changes observed when PE and LL are added.

Extrapolating from the results of Penfold et al. [27] the bulk solution structure in equilibrium with the surface is most likely vesicular, However, no strong correlation between the surface and solution structures were observed [27], and the equivalent solution properties were not explored further.

3.2. LAS-6/$CaCl_2$/phenylethanol

Model perfumes, PE or LL, were progressively added (as described in the Experimental Details) to surfaces at which equilibrium multilayer structures were established, such that the solution mole fraction changed from 100% LAS-6 to a mole ratio of 10/90 LAS-6/perfume, in steps of 10%. This was done for two different isotopic combinations, d-surfactant/h-perfume and h-surfactant/d-perfume in nrw, where in each case it is the deuterium labeled

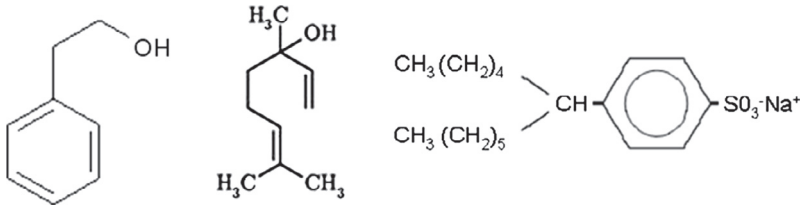

(a) Phenyl ethanol (b) Linalool (c) LAS-6

Fig. 1. Molecular structure of phenylethanol, linalool, and LAS-6.

component that is predominantly visible. The evolution in the NR data with solution composition for d-LAS-6/h-PE and h-LAS-6/d-PE is shown in Fig. 3.

The main features of the data are that for the d-LAS-6/h-PE combination (Fig. 3a) the Bragg peak is visible up to a surface composition of 10/90 mol ratio LAS-6/PE, and that the visibility of the Bragg peak increases with increasing amounts of PE added. For the isotopic combination h-LAS-6/d-PE (Fig. 3b) there is a Bragg peak visible over the composition range studied which has the same d spacing as seen for d-LAS-6/h-PE. Furthermore the visibility of the Bragg peak initially increases as the amount of PE added increases.

The transition from multilayer to monolayer adsorption is characterized by two features in the reflectivity profiles, the loss of Bragg peak and a significant change in the reflectivity at Q values below the Bragg peak. This is clearly shown in Fig. 3a in the data for 10/90 d-LAS-6/h-PE. In contrast the data for 10/90 h-LAS-6/d-PE (Fig. 3b) still shows some evidence of a Bragg peak in the data. This indicates some uncertainty in the composition at which the transition occurs, and the subsequent quantitative analysis is made for data in the composition range 20/80 to 90/10.

The data for compositions 20/80 to 90/10 are modeled with essentially the same parameters as was used for the LAS-6/$CaCl_2$ in the absence of perfume, that is, $d_1 = 17.5 \pm 0.5$, $d_2 = 14 \pm 0.5$, $N = 30 \pm 5$ and $\Delta Q = 0.1 \pm 0.02$, with only changes to ρ_1 and ρ_2. The variation in ρ_1 and ρ_2 values with composition for the two contrasts measured and listed in Table 2, and typical model fits are shown in Fig. 4 for 70/30 mol ratio LAS-6/PE.

It has previously been demonstrated at the interface [30] and in solution [9,11] that the more hydrophilic phenylethanol is preferentially located close to the headgroup region. Hence in the modeling of the data here it is assumed that the phenylethanol is in the region of the bilayer (d_2) occupied by the phenyl ring and headgroup. The data are well described by this assumption, and the variation in ρ_1 and ρ_2 in Table 2 with increasing amounts of added PE are consistent of with an increased incorporation of the PE into that region of the bilayer structure.

From the NR data for h-LAS-6/d-PE the contribution to the reflectivity is predominantly from the d-PE, but there will be a residual contribution from the h-LAS-6. The data and modeling are not sufficiently precise to estimate the amount of PE present in the multilayer accurately. However, making the approximation that for the h-LAS-6/d-PE data and model parameters $\Delta\rho$ ($\rho_2 - \rho_1$) represents the d-PE contribution then the amount of PE within the region of the bilayer defined by d_2 can be simply estimated (using $A = \sum b/d\Delta\rho$). Taking an average value for $\Delta\rho$ of 0.4×10^{-6} Å^{-2} (from Table 2) this gives an adsorbed amount/bilayer of $\sim 1.25 \times 10^{-10}$ mol cm^{-2}. This amount is broadly consistent with coadsorption of PE in the absence of $CaCl_2$ where only monolayer adsorption occurs [35]. Furthermore, assuming that the perfume is equally distributed within the whole bilayer stack, then the total adsorption is $\sim 40 \times 10^{-10}$ mol cm^{-2}. The model parameters in Table 2 show that in detail the amount of PE adsorbed increases with increasing amount of PE added. This is also evident qualitatively from the increased visibility of the Bragg peak with increasing amount of PE added, as shown in Fig. 3b. The change in $\Delta\rho$ shows that for a solution composition of 90/10 mol ratio LAS-6/PE to a 50/50 mol ratio the amount of PE adsorbed has increased by ~50%, and is then relatively constant up to a mole ratio of 20/80.

3.3. LAS-6/$CaCl_2$/linalool

A sequence of NR measurements, similar to those for LAS-6/PE, were also made for LAS-6/LL. The evolution in the NR data with solution composition for d-LAS-6/h-LL and h-LAS-6/d-LL are shown in Fig. 5. The data are broadly similar to that obtained for LAS-6/PE (see Fig. 3), but there are some notable differences. For the combination of d-LAS-6/h-LL (Fig. 5a) in nrw the visible Bragg peak at $Q \sim 0.2$ Å^{-1}, which characterizes the surface multilayer formation, decreases notably with increasing amounts of added LL. For solution compositions richer in LL than 40/60 mol ratio LAS-6/LL the Bragg peak is no longer visible, and the reflectivity at Q values below the Bragg peak changes markedly. This is consistent with only monolayer adsorption. This is also evident in the NR data for the combination h-LAS-6/d-LL in nrw (Fig. 5b). Taking into account the data for both d-LAS-6/h-LL and h-LAS-6/d-LL the transition from multilayer to monolayer adsorption occurs between compositions 40/60 and 50/50. These results compared to the results for LAS-6/PE imply that the incorporation of PE into the multilayer structure has a greater impact upon the sustaining the surface structure than LL. For the NR data for the combination h-LAS-6/d-LL the other significant difference, compared to LAS-6/PE, is that the Bragg peak is in general less visible. Qualitatively this would imply that that there is less LL incorporated into the multilayer structure than for PE.

The NR data for the LAS-6/LL mixtures in the composition range 50/50 to 90/10 are modeled using the same approach as applied earlier to the LAS-6/PE mixtures. The only difference is that, consistent with previous arguments about the location of the more hydrophobic perfumes, such as LL, in self-assembled surfactant structures [11], it is assumed that the LL is located within the alkyl chain region (d_1) of the bilayer structure. Representative model fits for 80/20 mol ratio LAS-6/LL are shown in Fig. 6, and the key model parameters are listed in Table 3. The basic model parameters for the LAS-6/LL mixtures are similar to those obtained for the LAS-6 and LAS-6/PE mixtures; that is, $d_1 = 17.5 \pm 0.5$ Å, $d_2 = 14 \pm 0.5$ Å, $N = 30 \pm 5$, $\Delta Q = 0.1 \pm 0.02$, and the ρ_1 and ρ_2 values are listed in Table 3.

The values of ρ_1 and ρ_2 in Table 3 reflect the incorporation of the LL in the alkyl chain region. Using the same arguments as discussed above for the LAS-6/PE data the amount of LL in the multilayer structure can be estimated from the $\Delta\rho$ value. Taking an average (from Table 3) $\sim 0.3 \times 10^{-6}$ Å^{-2} this gives an adsorbed amount for LL per bilayer $\sim 0.75 \times 10^{-10}$ mole cm^{-2} and a total adsorption within the entire multilayer stack $\sim 20 \times 10^{-10}$ mol cm^{-2}. Notably this is less than was observed for PE, and we will return to this point later.

As illustrated in Fig. 5, the NR data for solution compositions with LAS-6/LL mole ratios >50/50 are consistent with the adsorption of a mixed monolayer, ~20 Å thick, at the interface. Using the equation $d\rho = \frac{b_1}{A_1} + \frac{b_2}{A_2}$ for a binary mixture in nrw [31] and the values of dρ from the single layer model fits to the d-LAS-6/h-LL and h-LAS-6/d-LL data for the monolayer data provides an estimate of the amount of LAS-6 and LL at the interface in that region of solution compositions. Taking average values from the data for solution compositions of 30/70, 20/80 and 10/90 mol ratio gives a total adsorption (LAS-6 + LL) $\sim 5 \times 10^{-10}$ mol cm^{-2} and a surface composition (mole fraction of LL) ~0.45, and this is broadly similar to that previously reported for LL rich compositions in LAS-6/LL mixtures [35].

4. Discussion

The NR data show quite clearly that the surface multilayer structures established by the addition of $CaCl_2$ to the LAS-6 anionic surfactant are retained with the addition of two model perfumes, PE and LL; applied in-situ to the solutions. The surface multilayer structure is retained up to relatively high amounts of added perfume. In the case of PE the surface structure is retained up to a solution composition of at least 20/80 mol ratio LAS-6/PE. For the LL the surface structure is retained up to at least a 50/50 mol ratio

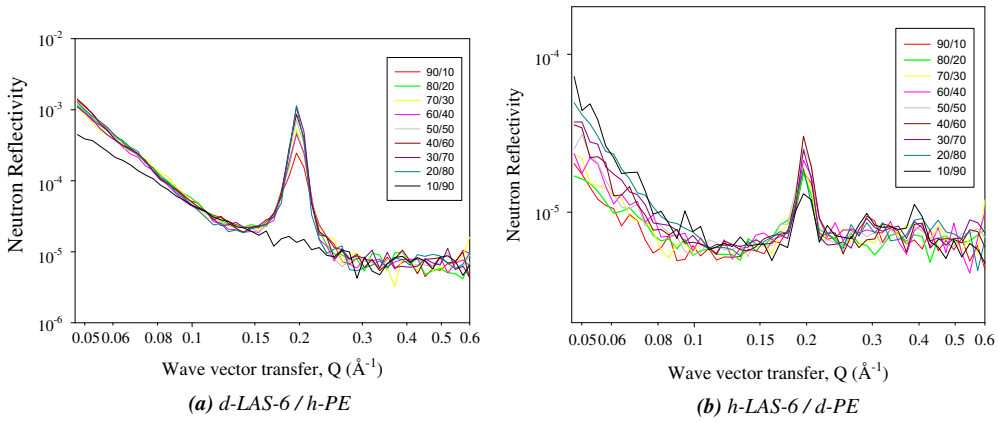

Fig. 3. NR data for 2 mM LAS-6/1 mM $CaCl_2$ in nrw, for (a) d-LAS-6/h-PE, (b) h-LAS-6/d-PE for LAS/PE compositions as shown in the legend. The data are plotted as lines for clarity, but the errors associated with the data are as indicated in Fig. 4.

Table 2
Key model parameters from analysis of 2 mM LAS-6/PE/1 mM $CaCl_2$ NR data. dh, hd refer to d-LAS-6/h-PE and h-LAS-6/d-PE respectively.

Mole ratio LAS-6/PE	Contrast	ρ_1 ($\pm 0.05 \times 10^{-6}$ Å^{-2})	ρ_2 ($\pm 0.05 \times 10^{-6}$ Å^{-2})
90/10	dh	5.2	3.3
	hd	0.2	0.6
80/20	dh	5.4	3.0
	hd	0.2	0.6
70/30	dh	5.3	2.9
	hd	0.3	0.7
60/40	dh	5.2	2.8
	hd	0.3	0.8
50/50	dh	5.2	2.7
	hd	0.3	0.9
40/60	dh	5.7	2.7
	hd	0.3	0.9
30/70	dh	5.6	2.5
	hd	0.3	0.9
20/80	dh	5.6	2.8
	hd	0.4	0.9

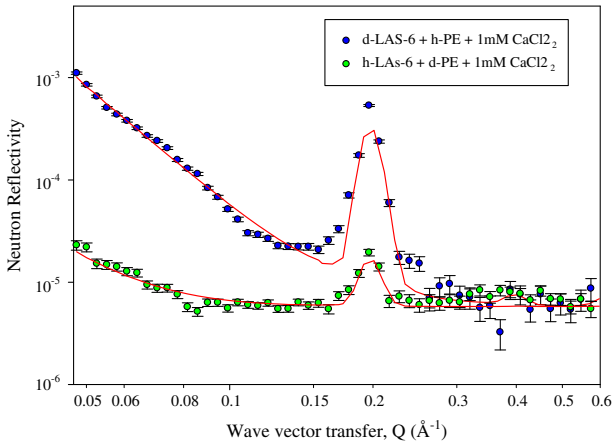

Fig. 4. NR data for 2 mM 70/30 mol ratio LAS-6/PE/1 mM $CaCl_2$, for (blue) d-LAS-6/h-PE, (green) h-LAS-6/d-PE. The solid lines are model calculations as described in the text and for the parameters in Table 2 and in the text. (For interpretation of the references to colour in this figure legend, the reader is referred to the web version of this article.)

LAS-6/LL solution composition. The two different 'contrasts' measured provide complementary information about the surface structure. The d-LAS-6/h-perfume measurements show predominantly the existence of the surface multilayer structure. Whereas the h-LAS-6/d-perfume data also provides evidence of the surface structure, but more importantly provides a direct measure of the amount of perfume within that surface structure.

The NR data in the absence of perfume are consistent with that previously reported for LAS-6/$CaCl_2$ [27]. The data have been modeled here by incorporating molecular constraints associated with the extended chain length, for a di-C_6 chain, dictating the alkyl chain region of the bilayer, and an incorporation of the phenyl ring into the headgroup region of the bilayer. This provides a good description of the data and scattering length densities for the two regions which are self-consistent.

The NR data with the addition of perfume are modeled assuming that the PE is predominantly in the headgroup region of the bilayer and that the LL is predominantly in the alkyl chain region. This is consistent with previous observations from the surface adsorption of surfactant/perfume mixtures [30] and on the impact of perfumes on surfactant self-assembly [9,26,36–38]. Furthermore, the variation in the scattering length densities of both the alkyl chain and headgroup regions, for d-LAS-6/h-perfume and h-LAS-6/d-perfume, is consistent with that interpretation.

What is notable in the data presented here is that the surface multilayer structure initially formed by LAS-6/$CaCl_2$ is retained to solution compositions richer in perfume for PE than for LL. This would seem initially in contradiction to the observations of the solution behavior. In solution the addition of PE predominantly into the palisade layer of micellar structures is observed [26,36–38], and is consistent with globular structures with a relatively high preferred curvature. In solution the addition of LL promotes a transition toward more planar self-assembled (lamellar) structures. This is a result of the more hydrophobic LL being more preferentially adsorbed further into the alkyl chain region [26,36–38]. The comparison between the surface and solution behavior is misleading, and what the NR data here are indicating is that it is easier to accommodate the addition of the PE up to relatively high amounts of added PE within the headgroup region without significant disruption to the multilayer structure. In contrast, solubilizing the LL (with almost twice the molecular volume) into the alkyl chain region results in a greater disruption to the surface structure. Furthermore this is compounded by the greater aqueous solubility of PE compared to LL. Hence PE can be more readily accommodated in solution than LL; and this will be important at these low surfactant concentrations (2 mM) where the concentration of aggregates in solution is relatively low. The values for the scattering length densities in Tables 2 and 3 show that the amount of perfume incorporated with the bilayer saturates at a solution

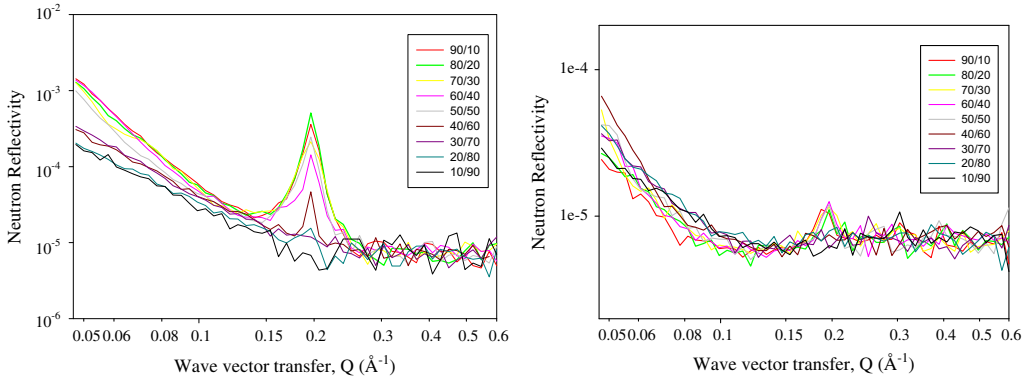

Fig. 5. NR data for 2 mM LAS-6/1 mM $CaCl_2$ in nrw, for (a) d-LAS-6/h-LL, (b) h-LAS-6/d-LL for LAS/LL compositions as shown in the legend. The data are plotted as lines for clarity, but the errors associated with the data are indicated in Fig. 6.

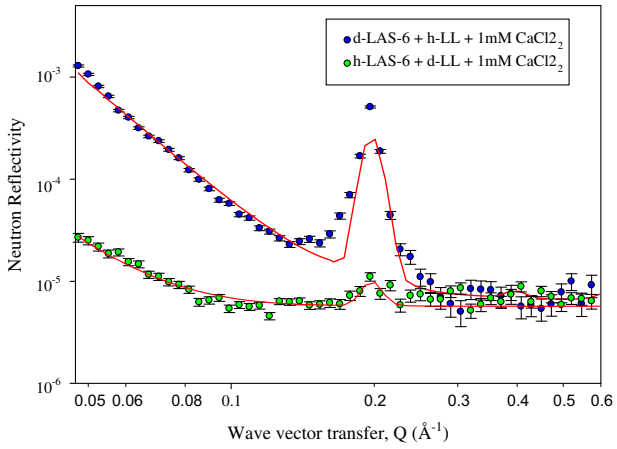

Fig. 6. NR data for 2 mM 80/20 mol ratio LAS-6/LL/1 mM $CaCl_2$, for (blue) d-LAS-6/h-LL, (green) h-LAS-6/d-LL. The solid lines are model calculations as described in the text and for the parameters in Table 3 and in the text. (For interpretation of the references to colour in this figure legend, the reader is referred to the web version of this article.)

Table 3
Key model parameters from analysis of 2 mM LAS-6/LL/1 mM $CaCl_2$ NR data. dh, hd refer to d-LAS-6/h-PE and h-LAS-6/d-PE respectively.

Mole ratio LAS-6/LL	Contrast	ρ_1 ($\pm 0.05 \times 10^{-6}$ Å^{-2})	ρ_2 ($\pm 0.05 \times 10^{-6}$ Å^{-2})
90/10	dh	5.5	3.4
	hd	0.7	0.4
80/20	dh	5.4	3.1
	hd	0.7	0.5
70/30	dh	4.9	3.0
	hd	0.8	0.5
60/40	dh	4.8	3.6
	hd	0.8	0.5
50/50	dh	4.3	2.7
	hd	0.8	0.5

composition of 50/50 mol ratio LAS-6/perfume for PE, and at a mole ratio of 70/30 for linalool.

The calculations (see earlier) based on the NR data for h-LAS-6/d-perfume show substantial adsorption of perfume into the multilayer structure. Within a single bilayer the amount of perfume coadsorbed is comparable to those observed in the co-adsorption with a LAS-6 monolayer at the surface, in the absence of $CaCl_2$ [26,35]. However, the number of bilayers in the surface structure means that the total amount of perfume within the surface region is substantially enhanced. As such this demonstrates that the surface multilayer structure provides a potentially promising environment for enhanced surface delivery and retention.

5. Conclusions

The NR results demonstrate the potential for enhanced delivery and retention of model perfumes to surfaces by incorporation into surface surfactant multilayer structures induced by multivalent ions [27,28]. It results in an enhanced amount of perfume at the interface by at least an order of magnitude compared to that co-adsorbed with a surfactant monolayer. The more hydrophobic linalool is predominantly solubilized into the alkyl chain regions in the surface multilayer structure. The more hydrophilic phenylethanol is predominantly solubilized into the headgroup region. These different locations are consistent with the observations associated with surfactant self-assembly and perfume solubilization [9,26,35]. The differences in location result in the surface multilayer structures existing over a wider range of surfactant/perfume compositions for phenylethanol than for linalool. This is in contrast to the trends observed in solution self-assembly [11], where linalool has a greater impact upon self-assembly than phenylethanol.

Acknowledgements

The provision of the beam time on the SURF reflectometer at ISIS and the expert assistance of the Instrument Scientist are acknowledged. The deuterated and hydrogeneous surfactants were provided by the Oxford Isotope Facility and Unilever Research and Development. The contributions of Steve Golding and Dave Thornthwaite in the synthesis of the deuterium labeled linalool were particularly important.

References

[1] S. Hermon, Fragrances in emulsion and surfactant systems, Cosmetics Toiletries Mag. 121 (2006) 59–67.
[2] S.E. Friberg, Fragrance compounds and amphiphilic association structures, Adv. Coll. Int. Sci. 75 (1998) 181–214.
[3] P. Aikens, S.E. Friberg, Organised assemblies in cosmetics and transdermal drug delivery, Curr. Opin. Coll. Int. Sci. 1 (1996) 672–676.
[4] Y. Tokuoka, H. Uchiyama, M. Abe, K. Ogino, Solubilisation of synthetic perfumes by nonionic surfactants, J. Coll. Int. Sci. 152 (1992) 402–409.
[5] M. Abe, K. Mizuguchi, Y. Kondo, K. Ogino, H. Uchiyama, J.F. Scamehorn, E.E. Tucker, S.D. Christian, Solubilisation of perfume compounds by pure and mixtures of surfactants, J. Coll. Int. Sci. 160 (1993) 16–23.

[6] Y. Kondo, M. Abe, K. Ogino, H. Uchiyama, J.F. Scamehorn, E.E. Tucker, S.D. Christian, Solubilisation of 2-phenylethanol in surfactant vesicles and micelles, Langmuir 9 (1993) 899–902.
[7] Y. Tokuoka, H. Uchiyama, M. Abe, Solubilisation of some synthetic perfumes by anionic and nonionic mixed surfactant systems, J. Phys. Chem. 98 (1994) 6167–6171.
[8] N. Kanei, Y. Tamura, H. Kunieda, Effects of types of perfume compounds on the hydrophilic–lipophilic balance temperature, J. Coll. Int. Sci. 218 (1999) 13–22.
[9] E. Fischer, W. Fieber, C. Navarro, H. Sommer, D. Benczedi, M. Velazco, M. Schonhoff, Partitioning and localization of fragrances in surfactant mixed micelles, J. Surf. Det. 12 (2009) 73–84.
[10] S.E. Friberg, Q. Yin, Vapour pressures of fragrance compounds during controlled evapouration, J. Disp. Sci. Technol. 20 (1999) 395–414.
[11] J. Penfold, I. Tucker, A. Green, D. Grainger, C. Jones, G. Ford, C. Roberts, J. Hubbard, J. Petkov, R.K. Thomas, I. Grillo, Impact of model perfumes on surfactant and mixed surfactant self-assembly, Langmuir 24 (2008) 12209–12220.
[12] S.C. Sharma, G.G. Warr, Phase behavior, self-assembly and emulsification of Tween 80/water mixtures with Limonene and perfluoromethyldecalin, Langmuir 28 (2012) 11707–11713.
[13] S. Magdassi, Delivery systems in cosmetics, Colloids Surf., A 123–124 (1997) 671–679.
[14] M.A. Tojer, L. Nordstirena, M. Nordin, M. Nyden, K. Holmberg, Encapsulation of actives for sustained release, PCCP 15 (2013) 17727–17741.
[15] E.D. Goddard, J.V. Gruber (Eds.), Principles of polymer science and technology in cosmetics and personal care, Marcel Dekker, NY, vol. 25, 1999 (Chapter 5).
[16] B.H. Lee, S.D. Christian, E.E. Tucker, J.F. Scamehorn, Effects of an anionic polyelectrolyte on the solubilisation of mono and dichlorophenols by aqueous solutions of N-hexadecylpyridinium chloride, Langmuir 7 (1991) 1332–1335.
[17] E.D. Goddard, R. Hannan, G.H. Matteson, Dye solubilisation by a cationic polymer/anionic surfactant system, J. Coll. Int. Sci. 60 (1977) 214–215.
[18] P.S. Leung, E.D. Goddard, C. Han, C.J. Glinka, The study of polycation–anionic surfactant systems, Coll. Surf. 13 (1985) 47–62.
[19] P. Somasundaran, S. Chakraborty, Q. Qiang, P. Deo, J. Wang, R. Zhang, Surfactants, polymers and their nanoparticles for personal care applications, J. Cosmet. Sci. 55 (2004) S1–S17.
[20] P.S. Given, Encapsulation of flavours in emulsions for beverages, Curr. Opin. Coll. Int. Sci. 14 (2009) 43–47.
[21] L.B. Petrovic, V.J. Sovilj, J.M. Katona, J.L. Milanovic, Influence of polymer–surfactant interactions on oil/water emulsion properties and microencapsulate formation, J. Coll. Int. Sci. 342 (2010) 333–339.
[22] M.A. Trojer, L. Nordstierna, M. Nordin, M. Nyden, K. Holmberg, Encapsulation of actives for sustained release, PCCP 15 (9) (2013) 17727–17741.
[23] B.P. Binks, P.D.I. Fletcher, B.L. Holt, P. Beaussoubre, K. Wong, Selective retardation of perfume oil evapouration from oil-in-water emulsions stabilized by either surfactant or nanoparticles, Langmuir 26 (2010) 18024–18030.
[24] R. Bradbury, J. Penfold, R.K. Thomas, I.M. Tucker, J.T. Petkov, C. Jones, Manipulating perfume delivery to the interface using polymer–surfactant interactions, J. Coll. Int. Sci., 2015 (in preparation).
[25] R. Bradbury, J. Penfold, R.K. Thomas, I.M. Tucker, J.T. Petkov, C. Jones, The impact of alkyl sulfate surfactant geometry and electrolyte on the co-adsorption of the anionic surfactants with model perfumes at the air–solution interface, J. Coll. Int. Sci. 403 (2013) 84–90.
[26] R.K. Thomas, J. Penfold, Multilayers of surfactant and mixtures of surfactants and electrolytes, polyelectrolytes, and proteins at the dilute air–water interface, Langmuir 31 (2015) 7440–7456.
[27] J. Penfold, R.K. Thomas, C.C. Dong, I. Tucker, K. Metcalfe, S. Golding, I. Grillo, Equilibrium surface adsorption behaviour in complex anionic/nonionic surfactant mixtures, Langmuir 23 (2007) 10140–10149.
[28] J.T. Petkov, I.M. Tucker, J. Penfold, R.K. Thomas, D.N. Petsev, C.C. Dong, S. Golding, I. Grillo, The impact of multivalent counterions Al^{3+} on the surface adsorption and self-assembly of the anionic surfactant alkyloxyethylene sulfate and anionic/nonionic surfactant mixtures, Langmuir 26 (2010) 16699–16709.
[29] http://www.isis.stfc.ac.uk/instruments/SURF/.
[30] J. Penfold, E. Staples, I. Tucker, L. Soubiran, R.K. Thomas, Comparison of the coadsorption of benzyl alcohol and phenylethanol with the cationic surfactant, hexadecyltrimethylammonium bromide, at the air–water interface, J. Coll. Int. Sci. 247 (2002) 397–403.
[31] J.R. Lu, R.K. Thomas, J. Penfold, Surfactant layers at the air–water interface: structure and composition, Adv. Coll. Int. Sci. 84 (2000) 142–304.
[32] S. Golding, D. Thornthwaite, private communication.
[33] I.M. Tidswell, B.M. Ocko, P.S. Pershan, S.R. Wasseman, G.M. Whitesides, J.D. Axe, X-ray specular reflection studies in silica coated by organic monolayers (alkylsiloxanes), Phys. Rev. B 41 (1990) 1111–1128.
[34] S.K. Sinha, M.K. Sanyal, S.K. Satija, C.F. Majkrzak, D.A. Neumann, G. Homma, S. Szpala, H. Gibaud, H. Morkov, X-ray scattering studies of surface roughness of GaAs/AlAs multilayers, Physica B 198 (1994) 72–77.
[35] R. Bradbury, J. Penfold, R.K. Thomas, I.M. Tucker, J.T. Petkov, C. Jones, Adsorption of model perfumes at the air–solution interface by coadsorption with an anionic surfactant, Langmuir 29 (2013) 3361–3369.
[36] R. Bradbury, J. Penfold, R.K. Thomas, I.M. Tucker, J.T. Petkov, C. Jones, I. Grillo, The impact of model perfumes on the self-assembly of the anionic surfactant sodium dodecyl-6-benzene sulfonate, Langmuir 29 (2013) 3234–3245.
[37] M. Kamada, S. Shimizu, K. Aramaki, Manipulation of the viscosity behavior of wormlike micellar gels by changing the molecular structure of added perfume, Colloids Surf., A (2014), http://dx.doi.org/10.1016/j.colsurfa.2014.01.003.
[38] I. Kayali, A. Khan, B. Lindman, Solubilisation and location of phenylalcohol, benzaldehyde and limonene in lamellar liquid crystals formed with block copolymers and water, J. Coll. Int. Sci. 297 (2006) 792–796.